ACS Partner Journal

POLYMER SCIENCE & TECHNOLOGY



https://pubs.acs.org/PolySciTech

Article

# Harnessing Self-Assembling Peptides on γδ T Cells to Enhance Anti-Tumor Immunity

Juan Liang,[#] Yu Fang,[#] Bihan Wu, Nan Kong, Sangshuang Li, Jianjun Cheng, Yan Xu,[*] and Huaimin Wang[*]

Cite This: https://doi.org/10.1021/polymscitech.5c00053

Read Online

ACCESS | Metrics & More | Article Recommendations | Supporting Information

**ABSTRACT:** γδ T cells possess significant anti-tumor potential; however, the expression of immune checkpoint molecules on tumor cells often leads to functional exhaustion of these T cells, resulting in variable outcomes in clinical trials. Targeting these immune checkpoints may alleviate the inhibitory effects of the tumor microenvironment on γδ T cell functionality. In this study, we developed a PD-L1-targeting peptide conjugated with maleimide, facilitating self-assembly on the surface of γδ T cells to form fibrous structures via Michael addition reactions with thiol groups on the cell membrane. Our findings demonstrate that this peptide effectively binds and self-assembles without impairing the proliferation or effector functions of γδ T cells. Notably, peptide-modified γδ T cells exhibited enhanced cytotoxic activity against tumor cells in vitro and significantly inhibited tumor growth in vivo. Furthermore, these modified γδ T cells promoted the infiltration of $CD8^+$ T cells and M1 macrophages into the tumor microenvironment. These results indicate that peptide-modified γδ T cells not only inhibit tumor progression but also mitigate the suppressive effects of the tumor microenvironment, thereby enhancing the synergistic anti-tumor responses of other immune cells. This research presents a straightforward and effective strategy for improving the immunosuppressive tumor microenvironment and augmenting the anti-tumor efficacy of γδ T cells.

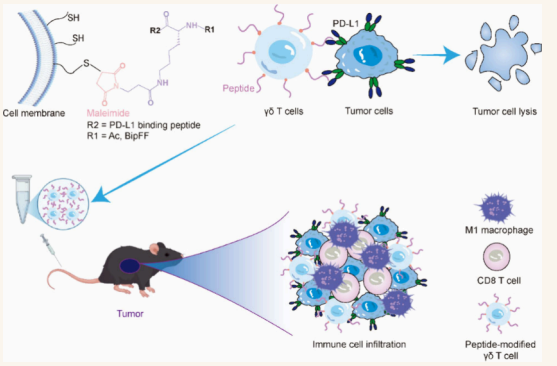


**KEYWORDS:** *Self-assembly, Peptide, Tumor microenvironment, Nanofiber, γδ T cells*



## INTRODUCTION

γδ T cells represent a unique subset of lymphocytes,[1] comprising approximately 1% to 10% of $CD3^+$ T cells in peripheral blood.[2] Although they are present in low abundance, they demonstrate significant anti-tumor efficacy in cancer immunotherapy. Firstly, γδ T cells are not constrained by major histocompatibility complex (MHC) molecules and do not require specific antigen presentation for activation.[3] They possess the capability to directly identify tumor cells via cell surface receptors, subsequently initiating cytotoxic responses.[4] This unique recognition mechanism imparts γδ T cells with extensive anti-tumor potential. Secondly, γδ T cells have the capacity to secrete a range of cytokines, including interferon-gamma (IFN-γ),[5] tumor necrosis factor-alpha (TNF-α),[6] and granulocyte-macrophage colony stimulating factor (GM-CSF),[6] among others. These cytokines play a crucial role in activating and augmenting the anti-tumor responses of other immune cells, such as natural killer (NK) cells,[7] $CD8^+$ T cells,[8] and macrophages.[8] Furthermore, γδ T cells exhibit memory-like characteristics[9] and long-term anti-tumor immune functions. Through their interactions with tumor cells, these cells can facilitate the generation of immune memory cells and sustain enduring anti-tumor immune responses. These attributes render γδ T cells essential effector cells in immunotherapy, presenting novel therapeutic opportunities for cancer patients. Despite comprehensive research demonstrating the potent anti-tumor effects of γδ T cells, patient responses to γδ T cell therapy in clinical settings display considerable heterogeneity.[10] This heterogeneity is partly attributable to the elevated expression of immune checkpoints within the tumor microenvironment.[11] Upon ligand binding, these checkpoints inhibit the immune response of γδ T cells, resulting in their functional exhaustion.[12−14] Therefore, it is imperative to devise the strategies to mitigate the influence of the tumor microenvironment on the functionality of γδ T cells, with the objective of enhancing the effectiveness of immunotherapy.

Immune checkpoint molecules within the tumor microenvironment, including PD-L1, CD24, and galectin 9, represent critical elements in tumor progression.[15] These checkpoints are markedly expressed on tumor cells and function to suppress the proliferation and activation of immune cells through interactions

Received: April 3, 2025
Revised: June 26, 2025
Accepted: June 27, 2025

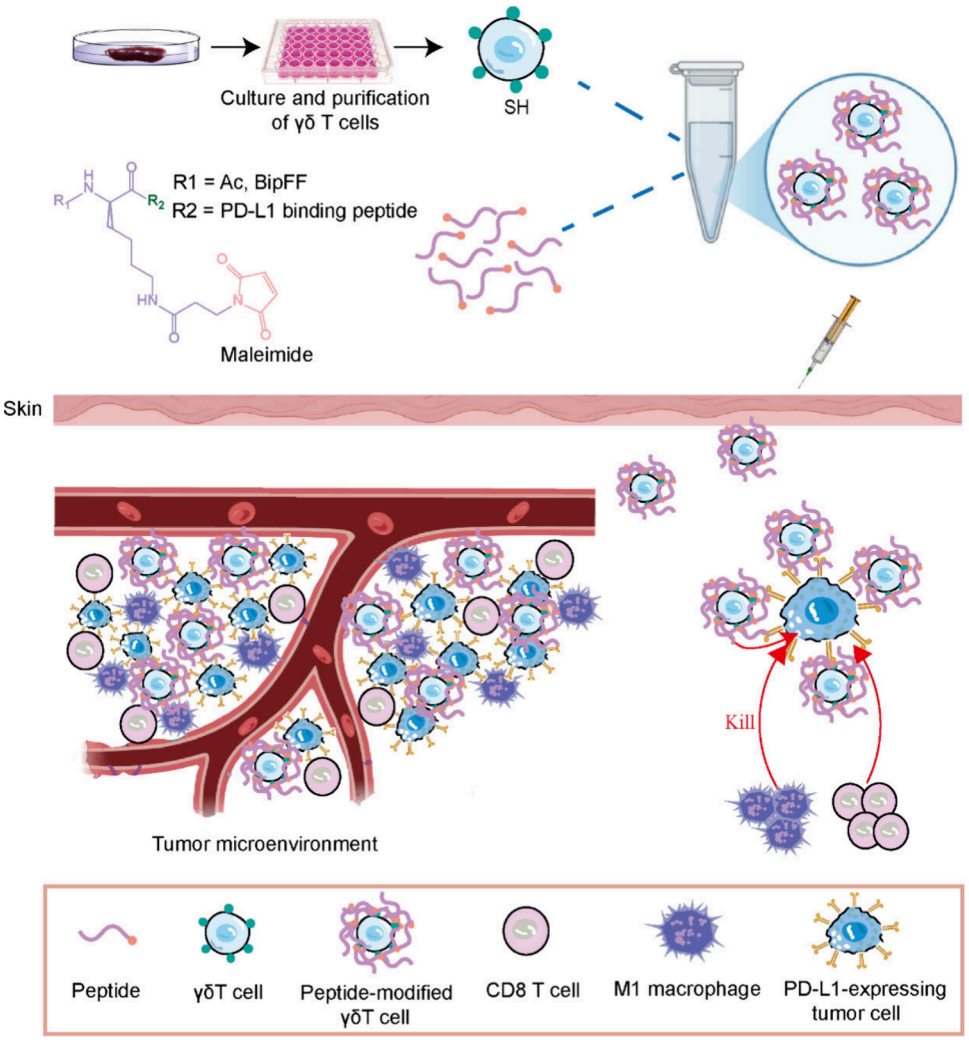


**Figure 1.** Schematic diagram of peptide-modified $\gamma\delta$ T cells targeting tumor PD-L1 to enhance anti-tumor efficacy. PD-L1-binding peptide-modified $\gamma\delta$ T cells specifically target tumor cells, reduce the suppressive influence of the tumor microenvironment, and enhance the infiltration of $\gamma\delta$ T cells, $CD8^+$ T cells, and M1 macrophages, thereby augmenting the synergistic anti-tumor efficacy of these immune cells.

with receptors on the immune cell surface.[16,17] Consequently, tumors are able to circumvent immune surveillance, thereby facilitating their growth and progression. Immune checkpoint therapy represents a novel anti-tumor approach that reinstates the capacity of immune cells to target tumors by inhibiting specific immune checkpoint molecules.[18] As of now, the United States Food and Drug Administration (FDA) has sanctioned the use of over 50 immune checkpoint antibodies for the treatment of various cancers.[19,20] Nonetheless, immune checkpoint antibody therapy continues to face several challenges, such as limited bioavailability, physiological barrier constraints, the development of drug resistance, and immune-related adverse effects.[21] Consequently, a small-molecule peptide that is readily synthesizable, exhibits high permeability, possesses low immunogenicity, and lacks Fc receptor-associated toxicity may represent the optimal alternative strategy for targeting immune checkpoint proteins (ICPs) to activate the immune system in the battle against cancer.[22] In prior researches, a variety of PD-L1-specific peptides were identified through phage display technology. These peptides demonstrated the ability to restore T cell activity and function when co-cultured with tumor cells in vitro, as well as effectively inhibit tumor growth in vivo.[23] Furthermore, peptides targeting emerging immune checkpoint proteins—including T cell immunoglobulin and mucin domain-containing protein 3 (TIM-3),[24] lymphocyte activation gene 3 (LAG-3),[25] and T cell immunoreceptor with Ig and ITIM domains (TIGIT)[26]—were also identified. These peptides augment T cell activity and demonstrate significant efficacy in inhibiting tumor growth in vivo. Due to the inherently short half-life of peptides in vivo and their susceptibility to protease-mediated degradation, conjugating them to a carrier molecule can significantly enhance their stability and bioavailability.[27] This approach not only extends their half-life but also augments their therapeutic efficacy.

In this study, we employed an approach that involved targeting tumor immune checkpoint molecules with peptides, enhancing the ability of $\gamma\delta$ T cells to overcome the inhibitory effects of the tumor microenvironment, and improving their anti-tumor efficacy. Specifically, we utilized a PD-L1-specific binding peptide that conjugated to the $\gamma\delta$ T cell surface through a Michael addition reaction between the maleimide on the peptide and the sulfhydryl groups present on the cell surface. The peptide was organized on the $\gamma\delta$ T cell surface through hydrophobic interactions and $\pi$-$\pi$ stacking, leading to the formation of nanofibers. Our in vitro investigations demonstrated that peptide assembly and modification did not influence


https://doi.org/10.1021/polymscitech.5c00053
Polym. Sci. Technol. XXXX, XXX, XXX−XXX

the proliferation or effector functions of γδ T cells. Importantly, γδ T cells modified with peptides exhibited enhanced cytotoxic effects against tumor cells. Simultaneously, the integration of the self-assembled moiety into the alternative peptide contributed to the stabilization of a β-sheet structure, promoting aggregation into various spatial configurations, multivalent interactions, and increased affinity. This modification enhanced the specificity and binding affinity for tumor cells. As expected, γδ T cells modified with self-assembling peptides further retarded tumor growth and reduced the suppressive impact of the tumor microenvironment on $CD8^+$ T cells and M1 macrophages in vivo. This modification promoted their infiltration into the tumor and facilitated a synergistic anti-tumor response (Figure 1). This work presents an innovative approach for non-genetic editing through straightforward and efficient peptide modification of γδ T cells, aimed at augmenting anti-tumor responses, which holds significant promise for the clinical application of γδ T cells in the future.

## MATERIALS AND METHODS

**Materials.** 6- to 8-week-old C57BL/6J female mice were purchased from the Laboratory Animal Resources Center at Westlake University. TCR $\delta^{-/-}$ mice were provided by Prof. Yan Xu (Jinan University, Guangzhou). Fmoc-amino acids were obtained from Shanghai Gil Biochemical Co., Ltd. The following reagents were purchased from BD Biosciences (USA): CFSE, PE rat anti-mouse CD8a, purified rat anti-mouse CD16/CD32, BD Cytofix/Cytoperm fixation/permeabilization, and BD Pharmingen Leukocyte Activation Cocktail. The LIVE/DEAD Fixable Blue Dead Cell Stain Kit was acquired from Invitrogen. Antibodies including PerCP/Cyanine5.5 anti-mouse CD3, FITC anti-mouse CD4, Brilliant Violet 421 anti-mouse TCR γ/δ, Brilliant Violet 650 anti-mouse CD45, Alexa Fluor® 700 anti-mouse CD107a (LAMP-1), Brilliant Violet 605 anti-mouse IFN-γ, Brilliant Violet 510 anti-mouse TNF-α, PE/Cyanine7 anti-human/mouse Granzyme B, Ultra-LEAF Purified anti-mouse CD28 and PE-conjugated anti-mouse TCR γδ antibody were sourced from BioLegend (San Diego, USA). InVivoMAb anti-mouse Vγ2 TCR was obtained from BioXCell (USA). Gibco RPMI-1640, Gibco DMEM, Oregon Green 488-conjugated malemide, Hoechst 33342 and CellMask Deep Red plasma membrane stains were acquired from Thermo Fisher (USA), while recombinant murine IL-2 was purchased from Peprotech (Hamburg, Germany). Red blood cell lysate was obtained from Biyuntian Company, and propidium iodide (PI) was sourced from Absin Co. (Shanghai, China). EasySep Ms PE Positive Selection Kit II was purchased from Stemcell (Canada).

**Synthesis of Peptides.** All peptides were synthesized using solid-phase peptide synthesis. Their purity was determined by analytical HPLC and verified by mass spectrometry in positive mode.

**TEM Characterizations.** TEM images were obtained using a FEI T12 microscope operated at an accelerating voltage of 120 kV. Standard TEM samples were prepared by dropping diluted products onto carbon-coated copper grids.

**Isolation of Murine Splenocytes and Culture of γδ T Cells.** To prepare γδ T antibody-coated 48-well plates, InVivoMAb anti-mouse Vγ2 TCR was incorporated into serum-free RPMI 1640 medium at a concentration of 10 μg/mL and thoroughly mixed. Subsequently, 100 μL of the prepared medium was dispensed into each well of a 48-well plate and incubated at 37°C for 4 h. Spleens from female C57BL/6 mice aged 6 to 8 weeks were homogenized and filtered through a 70-μm cell strainer. Erythrocytes were eliminated using a red blood cell lysis buffer, followed by two washes with PBS. The resulting cell pellet was resuspended in RPMI 1640 complete medium, adjusting the cell suspension to a concentration of $2 \times 10^6$ cells/mL.

The cell suspension was supplemented with recombinant mouse interleukin-2 (IL-2) at a concentration of 2 ng/mL and purified anti-mouse CD28 at 1 μg/mL. The medium from the 48-well plate was aspirated, and 500 μL of cell suspension was added to each well. The plate was incubated at 37°C, with the medium replaced every 2 days. On the sixth day, experiments utilizing magnetic bead cell sorting were performed to enrich γδ T cells. Initially, cells were harvested and resuspended in a sorting buffer at a concentration of $2 \times 10^8$ cells/mL. Then, they were incubated with anti-mouse CD16/CD32 (Fc block) for 10 min at room temperature, shielded from light. Subsequently, a PE-conjugated anti-mouse TCR γδ antibody was introduced and incubated at room temperature for 15 min under light-protected conditions. The cells were washed once with PBS and then resuspended in 1 mL of sorting buffer. 100 μL selection cocktail from EasySep Ms PE Positive Selection Kit II was added to the cell suspension and thoroughly mixed, followed by incubation at room temperature for 15 min. Subsequently, magnetic beads were introduced to the cell suspension after vortexing for 30 seconds. Following a 10 min incubation at room temperature, sorting buffer was added to reach a final volume of 2.5 mL. The tubes were then placed on a magnetic stand for 5 min. Unbound cells were gently aspirated. Finally, the bound cells were washed three times with sorting buffer to obtain purified γδ T cells.

**Peptide Modification of γδ T Cells.** The peptide was initially dissolved in water, and the solution's pH was adjusted to 6.5. γδ T cells were harvested and washed twice with PBS before resuspension at a concentration of $1 \times 10^6$ cells/mL. The peptide was then added to the cell suspension to achieve a final concentration of 50 μM and allowed to react at room temperature for 30 min. After incubation, the cells were washed once with PBS, and further experiments were conducted.

**Culture of MC38 Cell.** MC38 cells were cultured in DMEM medium supplemented with 10% heat-inactivated fetal bovine serum and 100 U/mL penicillin-streptomycin.

**Confocal Imaging.** Following a 30 min incubation of FITC-peptide with γδ T cells at room temperature in PBS, the cells were further incubated for an additional 24 h. After harvesting, the cells were washed once with PBS. The nuclei were counterstained using Hoechst 33342, and the cell membranes were labeled with CellMask Deep Red plasma membrane stains for 10 min. The cells underwent two additional washes with PBS before being placed onto glass slides. Mounting medium was applied, and coverslips were positioned over the samples. Confocal imaging was conducted using a Zeiss 980 microscope.

**Scanning Electron Microscopy (SEM).** For SEM sample preparation, the peptide was added to the γδ T cell suspension at a final concentration of 50 μM and incubated at room temperature for 30 min. The cells were then washed once with PBS. SEM samples were prepared according to standard protocols, and imaging was conducted using a field-emission scanning electron microscope (FEI Nova Nano SEM 450).

**Cell Viability Measurements.** γδ T cells and peptide-modified γδ T cells were harvested and washed twice with PBS. The cells were seeded at a density of 800,000 cells in 100 μL per well in 96-well plates. Cultures were maintained at 37°C in a humidified atmosphere with 5% $CO_2$ for 24 h. Cell viability was


https://doi.org/10.1021/polymscitech.5c00053
Polym. Sci. Technol. XXXX, XXX, XXX−XXX

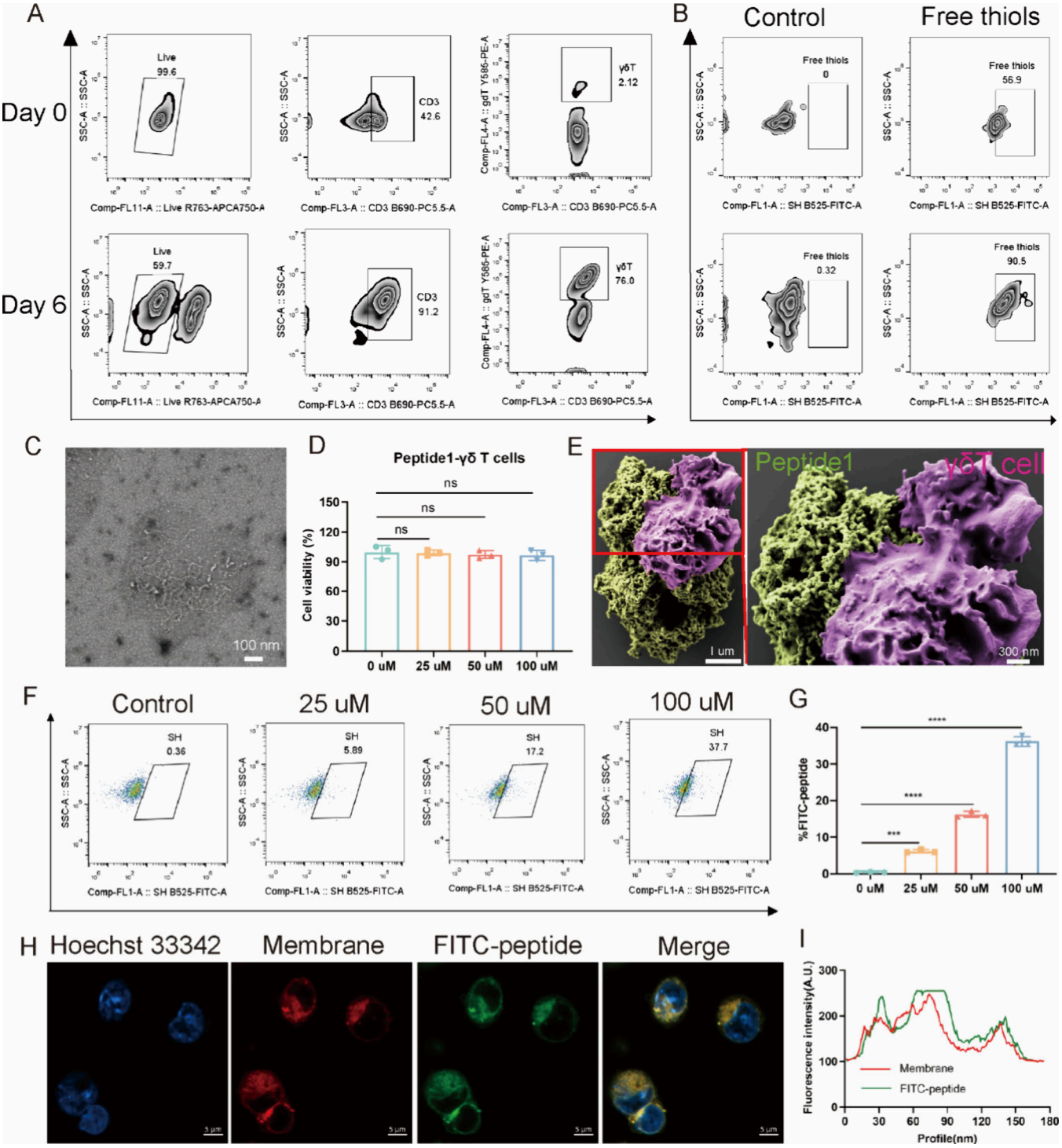


**Figure 2.** Peptide 1 reacted with sulfhydryl groups on the surface of $\gamma\delta$ T cells. (A) The proportion of $\gamma\delta$ T cells on days 0 and 6 in splenocyte cultures maintained in vitro was quantified using flow cytometry. (B) The levels of sulfhydryl groups on the surface of $\gamma\delta$ T cells on days 0 and 6 of in vitro culture were assessed via flow cytometry. (C) TEM image of Peptide 1. (D) Following a 24-hour incubation with Peptide 1, the viability of $\gamma\delta$ T cells was evaluated using the CCK8 assay. (E) SEM image of $\gamma\delta$ T cells treated with peptide 1 (100 uM). The pseudocolor in green represents peptide 1, while the purple color indicates the $\gamma\delta$T cell. (F) Flow cytometry plot showing the proportion of fluorescent peptide on the surface of $\gamma\delta$ T cells. (G) Bar graph depicting the percentage of fluorescent peptides on the surface of $\gamma\delta$ T cells. (H) Confocal images of FITC peptide-modified $\gamma\delta$ T cells taken after 24 h of culture. (I) Fluorescence intensity profiles of FITC-peptide interactions with $\gamma\delta$ T cell membranes. $p$ value, ns > 0.05, ***$p$ < 0.001, ****$p$ < 0.0001.

assessed using the CCK-8 assay according to the manufacturer's protocol.

**In Vitro Killing of Cancer Cells by $\gamma\delta$ T Cells.** MC38 cells were harvested, washed twice with PBS, and resuspended in serum-free RPMI 1640 medium. Carboxyfluorescein succinimidyl ester (CFSE) was added to the cell suspension to achieve a final concentration of 2 $\mu$M, followed by incubation at 37°C for 10 min. To terminate the staining process, pre-chilled complete


https://doi.org/10.1021/polymscitech.5c00053
Polym. Sci. Technol. XXXX, XXX, XXX−XXX

medium (three times the volume of the cell suspension) was added, and the mixture was placed on ice for 5 min. The cells were then washed twice with PBS and resuspended in medium for counting.

$\gamma\delta$ T cells and peptide-modified $\gamma\delta$ T cells were harvested and washed twice with PBS. CFSE-labeled MC38 cells were co-incubated with either $\gamma\delta$ T cells or peptide-modified $\gamma\delta$ T cells at a 1:10 ratio for 6 h at 37°C. After incubation, the cells were washed once with PBS, resuspended in PBS, and propidium iodide (PI) dye was added. Tumor cell mortality was evaluated using flow cytometric analysis.

**Flow Cytometry Analysis.** Standardized protocols were employed to stain cell surface markers. Cells were harvested and washed once with PBS. To prevent non-specific binding, anti-mouse CD16/CD32 (Fc block) was applied to block Fc receptors prior to staining. The LIVE/DEAD Fixable Blue Dead Cell Stain Kit (Invitrogen) was used to discriminate dead cells, with the incubation at 4 °C for 30 min. Following this, cells were washed again with PBS. Specific markers were then used to stain the cell surface: Brilliant Violet 650 anti-mouse CD45, PerCP/Cyanine5.5 anti-mouse CD3, FITC anti-mouse CD4, PE rat anti-mouse CD8a, and Brilliant Violet 421 anti-mouse TCR $\gamma/\delta$. Cells were incubated with these antibodies in PBS at 4 °C for 30 min and then washed once with PBS.

For intracellular staining, cells were fixed and permeabilized using the BD Cytofix/Cytoperm Plus Fixation/Permeabilization Kit. They were then stained with Brilliant Violet 785 anti-mouse IL-2, Brilliant Violet 605 anti-mouse IFN-$\gamma$, PE/Cyanine7 anti-mouse Granzyme B, Brilliant Violet 510 anti-mouse TNF-$\alpha$, Alexa Fluor® 700 anti-mouse CD107a (LAMP-1), and Pacific Blue anti-mouse Ki-67 antibody at 4 °C in the absence of light for 30 min. Afterward, the cells underwent one wash with a 1x washing buffer and an additional wash with PBS. Finally, the cells were analyzed using a Beckman CytoFlex LX flow cytometer.

The levels of sulfhydryl groups were detected by Flow cytometry. Cells were harvested and subjected to a single wash with PBS. Subsequently, the cells were incubated with a 0.1 $\mu$g/mL solution of Oregon Green 488-conjugated maleimide probe for 10 min at room temperature. Following incubation, the cells underwent two additional washes with PBS. Sulfhydryl levels on the cell surface were detected using flow cytometry.

The linking efficiency of FITC peptides on the cell surface was detected by Flow cytometry. Cells were collected, washed with the PBS and incubated with different concentrations of the FITC-peptide for 30 min at room temperature in the dark. The cells were then washed twice with PBS, and the FITC-peptide on the cell surface was detected by flow cytometry.

**Animal Experiments.** All animal experiments were conducted with the approval of the Ethical Committee for Animal Experimentation at Westlake University. Female TCR $\delta^{-/-}$ mice, aged 6 to 8 weeks, were used for in vivo studies, while female C57BL/6J mice of the same age range were employed for splenocyte extraction to culture $\gamma\delta$ T cells. On day 0, MC38 cells ($5 \times 10^5$) were subcutaneously injected into the right flank of each mouse. Body weight and tumor volume were assessed every 2 days post-tumor inoculation. Upon reaching an approximate tumor volume of 50 $mm^3$ on day 8, mice were randomly allocated into three groups of four mice each. A total of 4 million $\gamma\delta$ T cells or peptide-modified $\gamma\delta$ T cells were administered via intravenous injection through the tail vein every 3 days, culminating in five infusions. Mice were euthanized when tumor volume expanded to 1500 $mm^3$, followed by dissection.

Blood samples were collected via the orbital sinus prior to the initial cell infusion and again before euthanasia. Plasma was isolated, and inflammatory factors were analyzed using flow cytometry. The heart, liver, spleen, lungs, and kidneys were excised for hematoxylin and eosin (HE) staining. Immunofluorescent staining was conducted on tumor sections. Tumor-associated cells were isolated via enzymatic digestion of tumor tissues, followed by debris removal using a Percoll density gradient and lysis of red blood cells. The cells were then stained with antibodies and analyzed using the Beckman CytoFlex LX flow cytometer.

**Statistical Analysis.** Data were analyzed using GraphPad Prism 9 (GraphPad Software). Comparisons between two groups were conducted using the t-test. For comparisons among multiple groups, one-way repeated measures analysis was performed. A $p$-value of $<0.05$ was considered statistically significant.

## RESULTS AND DISCUSSION

**Peptide 1 Interacts with the Sulfhydryl Groups on the Surface of $\gamma\delta$ T Cells.** PD-L1 functions as an immune checkpoint for tumor cells by interacting with PD-1, thereby inhibiting immune cell activity. Recent studies have demonstrated that a peptide, identified and optimized through phage display (sequence: GQSEHHMRVYSF),[28] exhibits selective binding to PD-L1. This interaction effectively disrupts the PD-1/PD-L1 axis, leading to a marked increase in IFN-$\gamma$ secretion by $CD8^+$ T cells in human peripheral blood mononuclear cells. In addition, in vivo experiments have shown that this peptide substantially suppresses tumor progression in murine models of colorectal cancer and melanoma. Moreover, the D-type anti-PD-L1 peptide (NYSKPTDRQYHF)[29] has been engineered to form a novel peptide−polymer conjugate with polyethylene glycol (PEG) and MP9, serving as a systemic drug delivery vehicle characterized by PD-L1 targeting specificity and favorable pharmacokinetic properties. This conjugate demonstrates the ability to specifically target PD-L1 in tumor tissues and exhibits significant immunotherapeutic efficacy in murine models. Based on above consideration, we chose above two peptide sequences for the modification in our work.

Since the maleimide can form a stable linkage with cell surface sulfhydryl groups via the Michael addition reaction, we first assess the levels of sulfhydryl groups on the surface of $\gamma\delta$ T cells. Due to the low abundance of $\gamma\delta$ T cells in mice, it is necessary to expand these cells in vitro. To achieve this, mouse splenocytes were extracted and cultured for 6 days. The proportion of $\gamma\delta$ T cells was quantified using flow cytometry on both day 0 and day 6. The results indicated a significant increase in the proportion of $\gamma\delta$ T cells after 6 days of culture (Figure 2A). Concurrently, there was a notable increase in the levels of sulfhydryl groups on the surface of $\gamma\delta$ T cells (Figure 2B). After selecting a peptide with specific binding affinity to PD-L1 from existing literature, we synthesized it and conjugated it to maleimide, henceforth referred to as peptide 1 (S1). Transmission electron microscopy (TEM) analysis revealed that peptide 1 predominantly exists in an aggregated state (Figure 2C).

We also evaluated the potential cytotoxic effects of varying concentrations of peptide 1 on $\gamma\delta$ T cells. Purified $\gamma\delta$ T cells were exposed to peptide 1 at different concentrations and subsequently cultured for 24 h. Cellular activity measurement by CCK-8 assay demonstrated that peptide 1 could not significantly impact the activity of $\gamma\delta$ T cells (Figure 2D). To investigate the morphology of peptide 1 on the surface of $\gamma\delta$ T


https://doi.org/10.1021/polymscitech.5c00053
Polym. Sci. Technol. XXXX, XXX, XXX−XXX

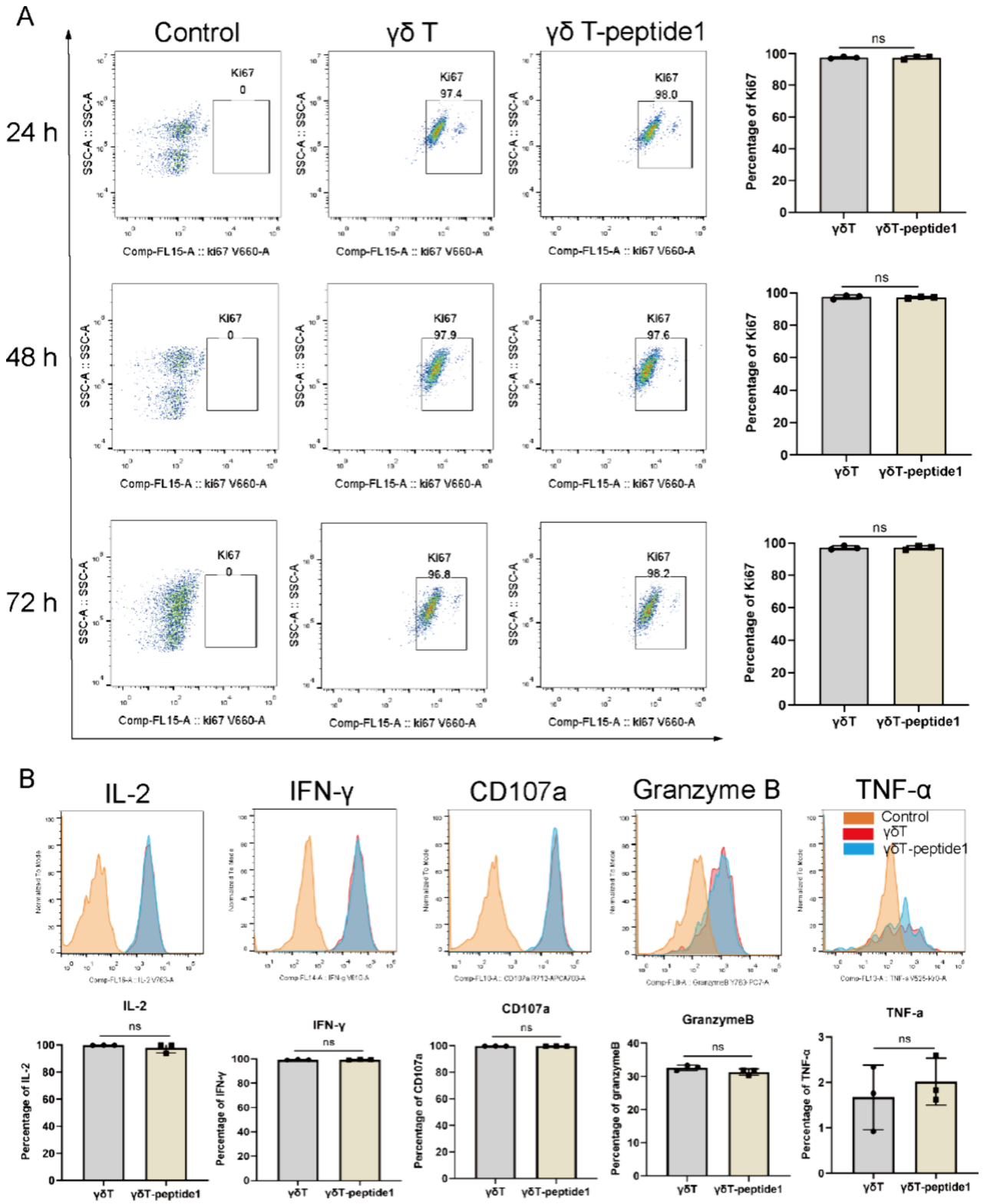


**Figure 3.** Modification of peptide 1 did not affect the proliferation and effector function of $\gamma\delta$ T cells. (A) The expression of Ki-67 in $\gamma\delta$ T cells was assessed following the culture of peptide-modified $\gamma\delta$ T cells for 24, 48, and 72 h, respectively. (B) The expression levels of IL-2, IFN-$\gamma$, CD107a, granzyme B, and TNF-$\alpha$ in $\gamma\delta$ T cells were evaluated after culturing peptide1-modified $\gamma\delta$ T cells for 72 h. $p$ value, ns > 0.05.

cells, we employed scanning electron microscopy (SEM). SEM results indicated that the peptide formed aggregates and adhered to the surface of the $\gamma\delta$ T cells (Figure 2E). To quantify the proportion of peptide attached to the cell surface at varying concentrations, we utilized flow cytometry to measure the fluorescence intensity of fluorescein isothiocyanate (FITC)-labeled peptide on the cell surface after treating $\gamma\delta$ T cells with FITC-peptide. Results showed that the intensity of FITC fluorescence on the surface of $\gamma\delta$ T cells increased with the increase of peptide concentrations (Figures 2F, G). Confocal


https://doi.org/10.1021/polymscitech.5c00053
Polym. Sci. Technol. XXXX, XXX, XXX−XXX

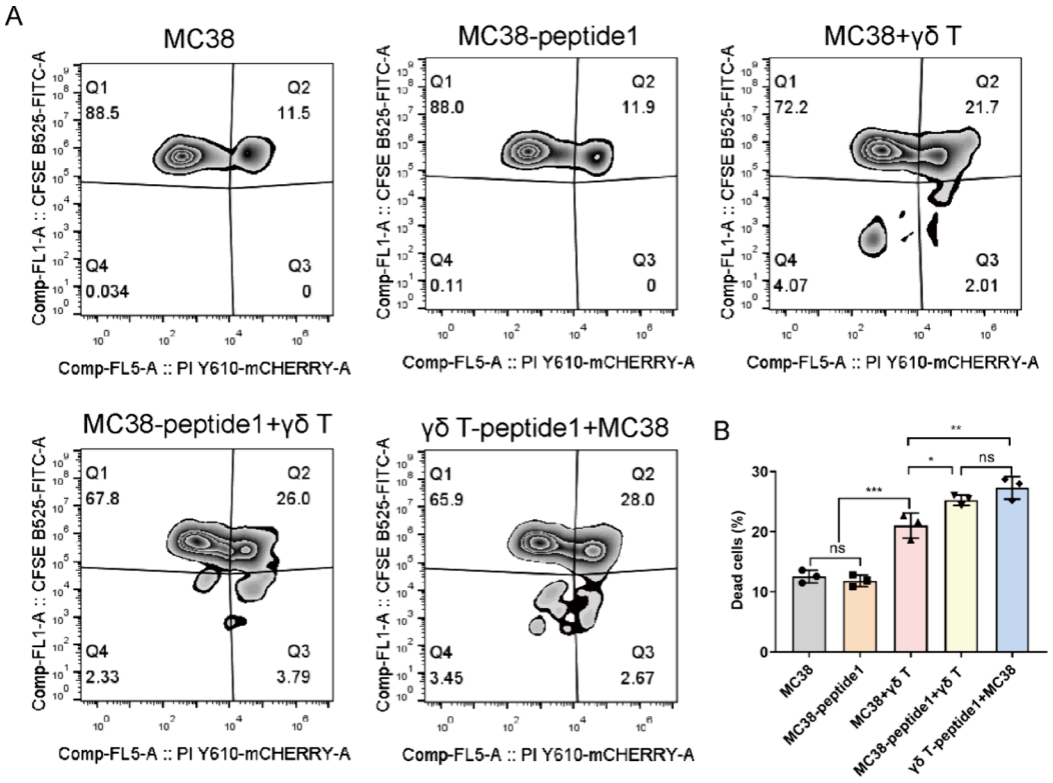


**Figure 4.** Modification of peptide 1 enhanced the ability of $\gamma\delta$ T cells to kill tumor cells in vitro. Following labeling with 5 $\mu$M CFSE, MC38 cells were subjected to modification with Peptide 1 alongside $\gamma\delta$ T cells. The experimental setup consisted of five distinct groups: MC38, MC38-Peptide 1, MC38 + $\gamma\delta$ T, MC38-Peptide 1 + $\gamma\delta$ T, and $\gamma\delta$ T-Peptide 1 + MC38. The MC38 cells and $\gamma\delta$ T cells were combined at a ratio of 1:10 and incubated for a duration of 6 h. Subsequently, the cells were stained with PI and analyzed using flow cytometry. (A) Flow cytometry diagram of tumor cell mortality. (B) A bar graph showing the percentage of dead tumor cells. $p$ value, *$p$ < 0.05, **$p$ < 0.01, ***$p$ < 0.001, ****$p$ < 0.0001.

microscopy analysis revealed the colocalization of the fluorescent peptide with the membrane of $\gamma\delta$ T cells (Figures 2H, I). These results suggest that maleimide-linked peptide 1 can be stably anchored to the surface of $\gamma\delta$ T cells.

**Modification of Peptide 1 and Its Impact on $\gamma\delta$ T Cell Function.** To investigate whether the modification of peptide 1 could affect the proliferation or effector function of $\gamma\delta$ T cells, we assessed Ki67 expression for cell proliferation. Following exposure of $\gamma\delta$ T cells to peptide 1, the cells were cultured further, and Ki67 expression was evaluated using flow cytometry at 24, 48, and 72 h. The results indicated that there is no significant difference in Ki67 expression between peptide 1-modified $\gamma\delta$ T cells and their unmodified counterparts (Figure 3A). Additionally, we evaluated the capacity of peptide 1-modified $\gamma\delta$ T cells to secrete key cytokines, including IL-2, IFN-$\gamma$, CD107a, Granzyme B, and TNF-$\alpha$, after a 72-hour culture period. These cytokines are crucial for the anti-tumor response. The findings showed that there is no significant difference in cytokine secretion between modified and unmodified $\gamma\delta$ T cells (Figure 3B). Overall, these results suggest that the proliferation and effector functions of $\gamma\delta$ T cells remain unaltered after modification.

**Modification of Peptide 1 Enhanced the Ability of $\gamma\delta$ T Cells to Kill Tumor Cells in Vitro.** We investigated whether $\gamma\delta$ T cells modified with peptide 1 could enhance their cytotoxic effect on tumor cells. MC38 cells were labeled with CFSE dye, and both MC38 cells and $\gamma\delta$ T cells were modified with peptide 1, respectively. The modified or unmodified MC38 cells and $\gamma\delta$ T cells were then co-cultured at a ratio of 1:10 and incubated for 6 h. Following incubation, propidium iodide (PI) dye was introduced to assess tumor cell viability via flow cytometry. The results indicated that the presence of $\gamma\delta$ T cells increased tumor cell mortality, which was further augmented when the $\gamma\delta$ T cells were modified with peptide 1 (Figure 4).

The MC38 tumor cells express the PD-L1 immune checkpoint. Targeting PD-L1 with peptide 1 partially reverses the inhibitory effects of MC38 cells on $\gamma\delta$ T cells, enhancing their cytotoxic activity. Flow cytometry shows that tumor cells have sulfhydryl groups that conjugate with FITC-peptide in a concentration-dependent manner (S8). After incubation with peptide 1, a covalent bond forms between the peptide and sulfhydryl groups through a maleimide linkage, inhibiting PD-L1's interaction with PD-1 on $\gamma\delta$ T cells and boosting their cytotoxic potential. However, the rapid proliferation of tumor cells leads to a dilution of the peptides, reducing therapeutic efficacy. Conjugating peptides to $\gamma\delta$ T cells can enhance targeting in vivo. Therefore, we conducted experiments using the peptide incubated with $\gamma\delta$ T cells.

**Peptide 2-Modified $\gamma\delta$ T Cells Delay Tumor Growth in Vivo.** To enhance the assembly capacity of peptides and their affinity for cell membranes, we employed BipFF,[30] a self-assembly motif to conjugate an additional peptide to the specific target PD-L1. This peptide, designated as peptide 2 (S2A). LC-MS analysis (S2B,C) and MALDI-TOF characterization (S2D) of peptide 2 were verified its identity and purity. TEM imaging revealed that peptide 2 self-assembles to form nanofibrous structure (S2E). To evaluate the potential cytotoxicity of peptide 2 against $\gamma\delta$ T cells, we performed a CCK-8 assay. Following exposure of purified $\gamma\delta$ T cells to varying concentrations of peptide 2 (25 $\mu$M, 50 $\mu$M, 100 $\mu$M), the


https://doi.org/10.1021/polymscitech.5c00053
Polym. Sci. Technol. XXXX, XXX, XXX−XXX

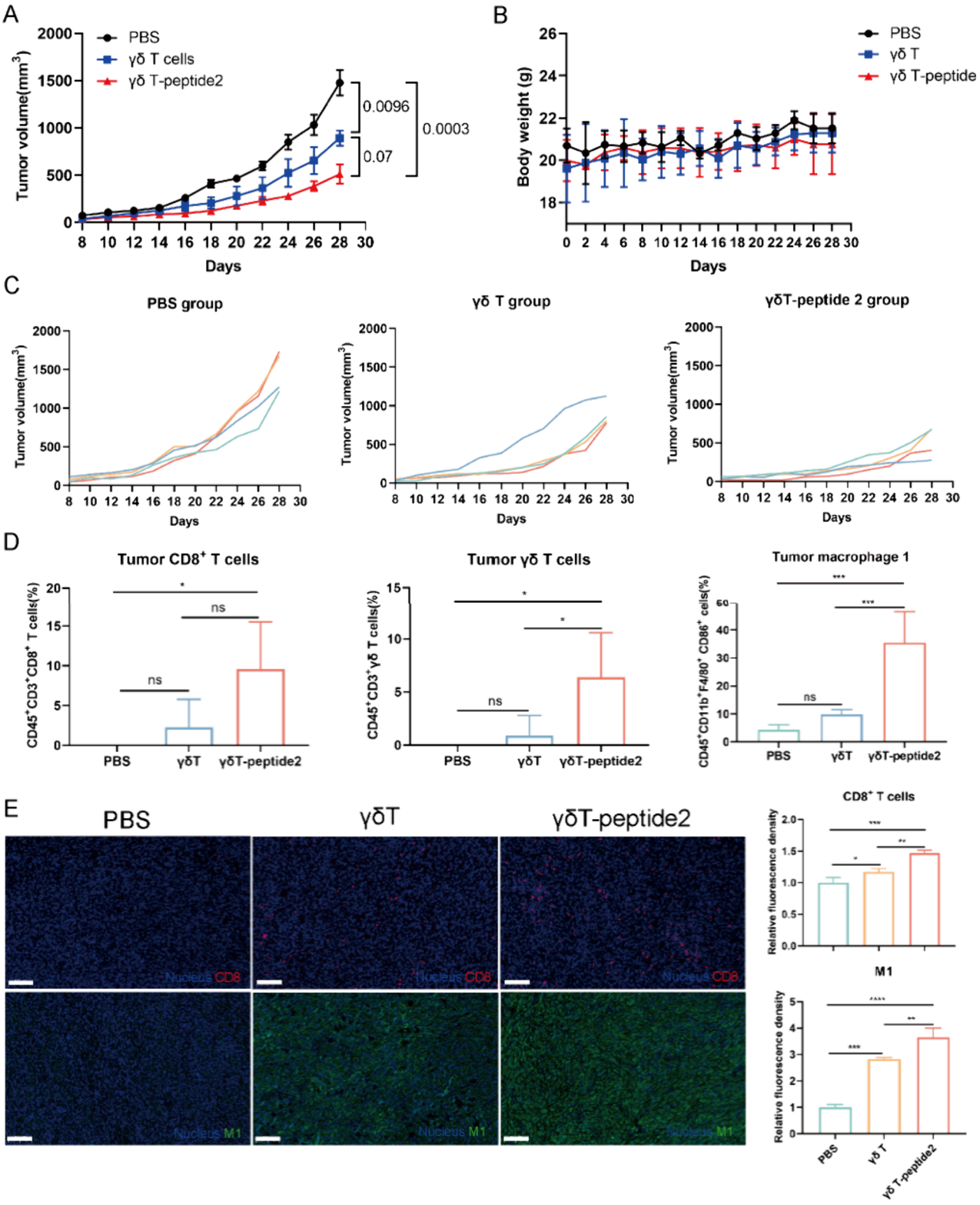


**Figure 5.** Peptide 2-modified $\gamma\delta$ T cells delay tumor growth in vivo. TCR $\delta^{-/-}$ C57BL/6J female mice were subcutaneously inoculated with MC38 cells. Upon tumor development to an approximate volume of 50 $mm^3$, the mice were randomly allocated into three groups, with each group comprising four mice ($n$ = 4). Tumor volume and body weight of the mice were systematically measured every 2 days. (A) Tumor growth curves. (B) Body weight curves of mice. (C) Tumor growth curves of each individual mouse from each group. (D) The proportions of $CD8^+$ T cells, $\gamma\delta$ T cells, and M1 macrophages in tumor were measured by flow cytometry. (E) Immunofluorescence staining was performed on $CD8^+$ T cells (red), M1 macrophages (green), and nuclei (blue), Scale bar: 100 $\mu$m. Histograms depict relative fluorescence intensity of $CD8^+$ T cells and M1 macrophages. $p$ value, *$p$ < 0.05, **$p$ < 0.01, ***$p$ < 0.001, ****$p$ < 0.0001.

cells were incubated for an additional 24 h. Subsequent assessment of cellular activity via the CCK-8 assay revealed that the peptide 2 did not significantly influence the activity of $\gamma\delta$ T cells (S2F). Concurrently, SEM results revealed the presence


https://doi.org/10.1021/polymscitech.5c00053
Polym. Sci. Technol. XXXX, XXX, XXX−XXX

of peptide aggregates associated with the γδ T cell membrane (S2G). In addition, this study sought to evaluate the cytotoxic effects of peptide 2-modified γδ T cells on tumor cells. Initially, MC38 cells were labeled with CFSE dye and subsequently combined with peptide 2-modified γδ T cells at a 1:10 ratio. Following a 6-hour incubation period, PI dye was introduced to assess tumor cell mortality via flow cytometry. The results indicated that peptide 2-modified γδ T cells significantly enhanced the tumor cell killing ratio, approximately doubling the efficacy compared to unmodified γδ T cells (S3).

We further investigate whether γδ T cells modified with peptide 2 exhibit enhanced anti-tumor efficacy in vivo. To mitigate the influence of γδ T cells in murine models, TCR $\delta^{-}/^{-}$ C57BL/6J female mice were subcutaneously inoculated with MC38 ($5 \times 10^5$) cells. Upon tumor growth reaching approximately 50 $mm^3$ by day 8, the mice were randomly allocated into three experimental groups: PBS, γδ T, and γδ T-peptide 2. All the groups were administered via tail vein injection into the mice assigned to each respective group. The mice received these cellular inoculations every 3 days, for a total of five administrations. Tumor volumes and body weights of the mice were assessed bi-daily. Mice were euthanized when tumor volumes reached approximately 1500 $mm^3$, at which point tumor samples were collected and measured.

Subsequently, we assessed the efficacy of peptide 2-modified γδ T cell infusions on tumor growth, body weight, and immune responses in vivo. Compared to the PBS control group, both γδ T cell and peptide 2-modified γδ T cell infusions resulted in a significant reduction in tumor growth (Figure 5A, C). Although the difference in tumor volume between the γδ T cell group and the peptide 2-modified γδ T cell group did not reach statistical significance, greater inhibition of tumor growth was observed in the peptide 2-modified group. In this study, γδ T cells were engineered with a peptide targeting the immune checkpoint PD-L1 to suppress tumor growth. Nevertheless, the tumor immunosuppressive microenvironment is a complex and dynamic entity. The therapeutic efficacy of this approach is constrained by other immunosuppressive elements within the tumor microenvironment, including additional immune checkpoints (such as galectin 9[31] and Siglec[32]) and immunosuppressive cells[33] (such as tumor-associated macrophages and myeloid-derived suppressor cells), as well as metabolites produced by tumor cells. These factors collectively impede the activity of immune cells in vivo, leading to an absence of significant differences in treatment outcomes between γδ T cells and peptide 2-modified γδ T cell group. Subsequent optimization experiments could focus on targeting multiple immunosuppressive pathways. In other words, the synthesis of peptides designed to target immune checkpoints and reverse the function of immunosuppressive cells, alongside the concurrent modification of γδ T cells by multiple peptides, aims to enhance anti-tumor efficacy.

Throughout the experimental period, no weight loss was noted in any of the three groups, suggesting that the cell treatment did not induce significant adverse effects (Figure 5B). An in-depth analysis of immune cell populations within the tumors revealed an elevated proportion of infiltrating $CD8^+$ T cells, γδ T cells, and M1 phenotype macrophages (Figure 5D). Immunofluorescence staining of tumor sections corroborated these findings, demonstrating enhanced infiltration of $CD8^+$ T cells and M1 macrophages within the tumor microenvironment (Figure 5E). These findings suggest that peptide 2-modified γδ T cell therapy effectively suppresses tumor growth and mitigates the immunosuppressive effects of the tumor microenvironment, thereby facilitating increased immune cell infiltration.

To evaluate the safety profile of peptide 2-modified γδ T cell therapy, we systematically recorded both systemic and localized safety parameters post-treatment. Following euthanasia, the heart, liver, spleen, lungs, and kidneys were harvested from each mouse and subjected to hematoxylin and eosin (H&E) staining. Comparative analysis revealed no significant histopathological differences among the tissues across the three experimental groups (S5). Additionally, we collected peripheral blood from the mice both before cell infusion and prior to euthanasia to detect inflammatory factors in plasma. We found no significant differences in inflammatory factor levels among the groups (S6). These results suggest that peptide 2-modified γδ T cell infusions did not cause organ damage or a cytokine storm, indicating that these infusions were biocompatible.

## CONCLUSION

Within the tumor microenvironment, immune checkpoint molecules significantly hinder the functionality of γδ T cells, resulting in their functional depletion and limiting the therapeutic efficacy observed in clinical trials. Addressing the challenges posed by these immune checkpoints is crucial for enhancing γδ T cell therapy. In this study, we employed innovative chemical modification techniques to conjugate PD-L1-specific binding peptides to the surface of γδ T cells. Our findings indicate that these modified γδ T cells retained their proliferation and effector functions while demonstrating targeted anti-tumor activity against PD-L1-expressing tumor cells.

A key aspect of our approach involved the self-assembly of peptide structures, which enhanced the specificity and stability of the modified γδ T cells. By utilizing self-assembled peptide constructs,[34−48] we achieved a more effective presentation of PD-L1 binding sites, facilitating improved targeting and engagement with tumor cells. This self-assembly not only reinforces the therapeutic potential of the γδ T cells but also provides a robust platform for further modifications, allowing the incorporation of additional functional elements to amplify the anti-tumor response. Importantly, the peptide-modified γδ T cells increased cytotoxicity against tumor cells and promoted the infiltration of $CD8^+$ T cells and M1 macrophages into the tumor microenvironment. This modulation of immune checkpoints, particularly through the targeting of PD-L1, mitigates the suppressive effects of the tumor microenvironment and enhances the synergistic anti-tumor responses of other immune cells.

These results underscore an effective strategy for alleviating immunosuppressive conditions within the tumor microenvironment, thereby improving the anti-tumor efficacy of γδ T cells. The application of peptide self-assembly in this context not only enhances the specificity of γδ T cell therapy but also opens new avenues for the development of multifunctional immunotherapeutic strategies. Future research should focus on validating this approach in clinical settings, with an emphasis on elucidating the underlying mechanisms and evaluating its impact on diverse immune cell populations.

## ASSOCIATED CONTENT

### Supporting Information

The Supporting Information is available free of charge at https://pubs.acs.org/doi/10.1021/polymscitech.5c00053.



https://doi.org/10.1021/polymscitech.5c00053
Polym. Sci. Technol. XXXX, XXX, XXX−XXX

Additional experiments were conducted, encompassing peptide characterization, LC-MS spectra, MALDI-TOF mass spectra, TEM and SEM imaging, determination of peptide critical micelle concentration, flow cytometry analysis, assessment of peptide cytotoxicity, evaluation of inflammatory factor release in mice, and H&E staining imaging (PDF)

## AUTHOR INFORMATION


### Corresponding Authors

**Huaimin Wang** − *Department of Chemistry, School of Science, Westlake University, Hangzhou, Zhejiang 310024, China;* orcid.org/0000-0002-8796-0367; Email: wanghuaimin@westlake.edu.cn

**Yan Xu** − *Biomedical Translational Research Institute and School of Pharmacy, Jinan University, Guangzhou 510632, China*; Email: sau_xuyan@163.com

### Authors

**Juan Liang** − *Department of Chemistry, School of Science, Westlake University, Hangzhou, Zhejiang 310024, China*

**Yu Fang** − *Department of Chemistry, School of Science, Westlake University, Hangzhou, Zhejiang 310024, China*

**Bihan Wu** − *Department of Chemistry, School of Science, Westlake University, Hangzhou, Zhejiang 310024, China*

**Nan Kong** − *Department of Chemistry, School of Science, Westlake University, Hangzhou, Zhejiang 310024, China*

**Sangshuang Li** − *Department of Chemistry, School of Science, Westlake University, Hangzhou, Zhejiang 310024, China*

**Jianjun Cheng** − *School of Engineering, Westlake University, Hangzhou, Zhejiang 310024, China;* orcid.org/0000-0003-2561-9291

Complete contact information is available at: https://pubs.acs.org/10.1021/polymscitech.5c00053


### Author Contributions

[#]J.L. and Y.F. contributed equally. H.M.W. supervised the research project. J.L. conducted the experiments and collected the data. Y.F. was responsible for synthesis of peptides as well as conducting certain cellular and animal experiments. N.K. and S.S.L. contributed to additional cellular experiments. Y.X. supplied TCR $\delta^{-/-}$ mice and offered some experimental guidance. J.J.C. provided intellectual support and revised the original work. J.L. and H.M.W. performed data analysis and drafted the manuscript, incorporating feedback from all co-authors. All authors reviewed and approved the final manuscript.

### Notes

The authors declare no competing financial interest.

## ACKNOWLEDGMENTS

This project was supported by the National Natural Science Foundation of China (U24A2076, 82272145) and the Foundation of Westlake University. We thank the Instrumentation and Service Center for Molecular Sciences, Instrumentation and Service Center for Physical Sciences, General Equipment Core Facility, Biomedical Research Core Facilities, and Laboratory Animal Resource Center at Westlake University for the assistance with measurements.

## REFERENCES


(1) Thomas, P.; Paris, P.; Pecqueur, C. Arming V$\delta$2 T Cells with Chimeric Antigen Receptors to Combat Cancer. *Clin. Cancer Res.* **2024**, *30* (15), 3105−3116.

(2) Kabelitz, D.; Serrano, R.; Kouakanou, L.; Peters, C.; Kalyan, S. Cancer immunotherapy with $\gamma\delta$ T cells: many paths ahead of us. *Cell. Mol. Immunol.* **2020**, *17* (9), 925−939.

(3) Yang, Y.; Li, L.; Yuan, L.; Zhou, X.; Duan, J.; Xiao, H.; Cai, N.; Han, S.; Ma, X.; Liu, W.; Chen, C. C.; Wang, L.; Li, X.; Chen, J.; Kang, N.; Chen, J.; Shen, Z.; Malwal, S. R.; Liu, W.; Shi, Y.; Oldfield, E.; Guo, R. T.; Zhang, Y. A Structural Change in Butyrophilin upon Phosphoantigen Binding Underlies Phosphoantigen-Mediated V$\gamma$9V$\delta$2 T Cell Activation. *Immunity* **2019**, *50* (4), 1043−1053.e5.

(4) Silva-Santos, B.; Mensurado, S.; Coffelt, S. B. $\gamma\delta$ T cells: pleiotropic immune effectors with therapeutic potential in cancer. *Nat. Rev. Cancer* **2019**, *19* (7), 392−404.

(5) Gao, Y.; Yang, W.; Pan, M.; Scully, E.; Girardi, M.; Augenlicht, L. H.; Craft, J.; Yin, Z. Gamma delta T cells provide an early source of interferon gamma in tumor immunity. *J. Exp. Med.* **2003**, *198* (3), 433−42.

(6) Gao, Z.; Bai, Y.; Lin, A.; Jiang, A.; Zhou, C.; Cheng, Q.; Liu, Z.; Chen, X.; Zhang, J.; Luo, P. Gamma delta T-cell-based immune checkpoint therapy: attractive candidate for antitumor treatment. *Mol. Cancer* **2023**, *22* (1), 31.

(7) Maniar, A.; Zhang, X.; Lin, W.; Gastman, B. R.; Pauza, C. D.; Strome, S. E.; Chapoval, A. I. Human gammadelta T lymphocytes induce robust NK cell-mediated antitumor cytotoxicity through CD137 engagement. *Blood* **2010**, *116* (10), 1726−33.

(8) Xiang, Z.; Tu, W. Dual Face of V$\gamma$9V$\delta$2-T Cells in Tumor Immunology: Anti- versus Pro-Tumoral Activities. *Front. Immunol.* **2017**, *8*, 1041.

(9) Sheridan, B. S.; Romagnoli, P. A.; Pham, Q. M.; Fu, H. H.; Alonzo, F., 3rd; Schubert, W. D.; Freitag, N. E.; Lefrançois, L. $\gamma\delta$ T cells exhibit multifunctional and protective memory in intestinal tissues. *Immunity* **2013**, *39* (1), 184−95.

(10) Hu, Y.; Hu, Q.; Li, Y.; Lu, L.; Xiang, Z.; Yin, Z.; Kabelitz, D.; Wu, Y. $\gamma\delta$ T cells: origin and fate, subsets, diseases and immunotherapy. *Signal Transduction Targeted Ther.* **2023**, *8* (1), 434.

(11) Liu, J.; Wu, M.; Yang, Y.; Wang, Z.; He, S.; Tian, X.; Wang, H. $\gamma\delta$ T cells and the PD-1/PD-L1 axis: a love-hate relationship in the tumor microenvironment. *J. Transl. Med.* **2024**, *22* (1), 553.

(12) Rancan, C.; Arias-Badia, M.; Dogra, P.; Chen, B.; Aran, D.; Yang, H.; Luong, D.; Ilano, A.; Li, J.; Chang, H.; Kwek, S. S.; Zhang, L.; Lanier, L. L.; Meng, M. V.; Farber, D. L.; Fong, L. Exhausted intratumoral V$\delta$2(−) $\gamma\delta$ T cells in human kidney cancer retain effector function. *Nat. Immunol.* **2023**, *24* (4), 612−624.

(13) Liang, F.; Zhang, C.; Guo, H.; Gao, S. H.; Yang, F. Y.; Zhou, G. B.; Wang, G. Z. Comprehensive analysis of BTN3A1 in cancers: mining of omics data and validation in patient samples and cellular models. *FEBS Open Bio* **2021**, *11* (9), 2586−2599.

(14) Yu, L.; Wang, Z.; Hu, Y.; Wang, Y.; Lu, N.; Zhang, C. Tumor-infiltrating gamma delta T-cells reveal exhausted subsets with remarkable heterogeneity in colorectal cancer. *Int. J. Cancer* **2023**, *153* (9), 1684−1697.

(15) de Visser, K. E.; Joyce, J. A. The evolving tumor microenvironment: From cancer initiation to metastatic outgrowth. *Cancer Cell* **2023**, *41* (3), 374−403.

(16) Sharma, P.; Siddiqui, B. A.; Anandhan, S.; Yadav, S. S.; Subudhi, S. K.; Gao, J.; Goswami, S.; Allison, J. P. The Next Decade of Immune Checkpoint Therapy. *Cancer Discov* **2021**, *11* (4), 838−857.

(17) Kennedy, A.; Waters, E.; Rowshanravan, B.; Hinze, C.; Williams, C.; Janman, D.; Fox, T. A.; Booth, C.; Pesenacker, A. M.; Halliday, N.; Soskic, B.; Kaur, S.; Qureshi, O. S.; Morris, E. C.; Ikemizu, S.; Paluch, C.; Huo, J.; Davis, S. J.; Boucrot, E.; Walker, L. S. K.; Sansom, D. M. Differences in CD80 and CD86 transendocytosis reveal CD86 as a key target for CTLA-4 immune regulation. *Nat. Immunol.* **2022**, *23* (9), 1365−1378.




https://doi.org/10.1021/polymscitech.5c00053
*Polym. Sci. Technol.* XXXX, XXX, XXX−XXX

(18) Butterfield, L. H.; Najjar, Y. G. Immunotherapy combination approaches: mechanisms, biomarkers and clinical observations. *Nat. Rev. Immunol.* **2024**, *24* (6), 399−416.
(19) Vaddepally, R. K.; Kharel, P.; Pandey, R.; Garje, R.; Chandra, A. B. Review of Indications of FDA-Approved Immune Checkpoint Inhibitors per NCCN Guidelines with the Level of Evidence. *Cancers (Basel)* **2020**, *12*, 738.
(20) Hargadon, K. M.; Johnson, C. E.; Williams, C. J. Immune checkpoint blockade therapy for cancer: An overview of FDA-approved immune checkpoint inhibitors. *Int. Immunopharmacol.* **2018**, *62*, 29−39.
(21) Sun, Q.; Hong, Z.; Zhang, C.; Wang, L.; Han, Z.; Ma, D. Immune checkpoint therapy for solid tumours: clinical dilemmas and future trends. *Signal Transduction Targeted Ther.* **2023**, *8* (1), 320.
(22) Islam, M. K.; Stanslas, J. Peptide-based and small molecule PD-1 and PD-L1 pharmacological modulators in the treatment of cancer. *Pharmacol. Ther.* **2021**, *227*, 107870.
(23) Gurung, S.; Khan, F.; Gunassekaran, G. R.; Yoo, J. D.; Poongkavithai Vadevoo, S. M.; Permpoon, U.; Kim, S. H.; Kim, H. J.; Kim, I. S.; Han, H.; Park, J. H.; Kim, S.; Lee, B. Phage display-identified PD-L1-binding peptides reinvigorate T-cell activity and inhibit tumor progression. *Biomaterials* **2020**, *247*, 119984.
(24) Zhong, T.; Zhao, C.; Wang, S.; Tao, D.; Ma, S.; Shou, C. The biologically functional identification of a novel TIM3-binding peptide P26 in vitro and in vivo. *Cancer Chemother. Pharmacol.* **2020**, *86* (6), 783−792.
(25) Zhai, W.; Zhou, X.; Wang, H.; Li, W.; Chen, G.; Sui, X.; Li, G.; Qi, Y.; Gao, Y. A novel cyclic peptide targeting LAG-3 for cancer immunotherapy by activating antigen-specific CD8(+) T cell responses. *Acta Pharm. Sin. B* **2020**, *10* (6), 1047−1060.
(26) Zhou, X.; Zuo, C.; Li, W.; Shi, W.; Zhou, X.; Wang, H.; Chen, S.; Du, J.; Chen, G.; Zhai, W.; Zhao, W.; Wu, Y.; Qi, Y.; Liu, L.; Gao, Y. A Novel d-Peptide Identified by Mirror-Image Phage Display Blocks TIGIT/PVR for Cancer Immunotherapy. *Angew. Chem. Int. Ed.* **2020**, *59* (35), 15114−15118.
(27) Vadevoo, S. M. P.; Gurung, S.; Lee, H. S.; Gunassekaran, G. R.; Lee, S. M.; Yoon, J. W.; Lee, Y. K.; Lee, B. Peptides as multifunctional players in cancer therapy. *Exp. Mol. Med.* **2023**, *55* (6), 1099−1109.
(28) Li, W.; Zhu, X.; Zhou, X.; Wang, X.; Zhai, W.; Li, B.; Du, J.; Li, G.; Sui, X.; Wu, Y.; Zhai, M.; Qi, Y.; Chen, G.; Gao, Y. An orally available PD-1/PD-L1 blocking peptide OPBP-1-loaded trimethyl chitosan hydrogel for cancer immunotherapy. *J. Controlled Release* **2021**, *334*, 376−388.
(29) Lu, L.; Zhang, H.; Zhou, Y.; Lin, J.; Gao, W.; Yang, T.; Jin, J.; Zhang, L.; Nagle, D. G.; Zhang, W.; Wu, Y.; Chen, H.; Luan, X. Polymer chimera of stapled oncolytic peptide coupled with anti-PD-L1 peptide boosts immunotherapy of colorectal cancer. *Theranostics* **2022**, *12* (7), 3456−3473.
(30) Chen, D.; Zhou, Z.; Kong, N.; Xu, T.; Liang, J.; Xu, P.; Yao, B.; Zhang, Y.; Sun, Y.; Li, Y.; et al. Inhalable SPRAY nanoparticles by modular peptide assemblies reverse alveolar inflammation in lethal Gram-negative bacteria infection. *Sci. Adv.* **2024**, *10* (37), No. eado1749.
(31) Schlichtner, S.; Yasinska, I. M.; Lall, G. S.; Berger, S. M.; Ruggiero, S.; Cholewa, D.; Aliu, N.; Gibbs, B. F.; Fasler-Kan, E.; Sumbayev, V. V. T lymphocytes induce human cancer cells derived from solid malignant tumors to secrete galectin-9 which facilitates immunosuppression in cooperation with other immune checkpoint proteins. *J. immunotherap. cancer* **2023**, *11* (1), e005714.
(32) van de Wall, S.; Santegoets, K. C. M.; van Houtum, E. J. H.; Büll, C.; Adema, G. J. Sialoglycans and Siglecs Can Shape the Tumor Immune Microenvironment. *Trends Immunol.* **2020**, *41* (4), 274−285.
(33) Fan, Q.; Zuo, J.; Tian, H.; Huang, C.; Nice, E. C.; Shi, Z.; Kong, Q. Nanoengineering a metal-organic framework for osteosarcoma chemo-immunotherapy by modulating indoleamine-2,3-dioxygenase and myeloid-derived suppressor cells. *J. Exp. Clin. Cancer Res.* **2022**, *41* (1), 162.
(34) Wu, B.; Liang, J.; Yang, X.; Fang, Y.; Kong, N.; Chen, D.; Wang, H. A programmable peptidic hydrogel adjuvant for personalized immunotherapy in resected stage tumors. *J. Am. Chem. Soc.* **2024**, *146* (12), 8585−8597.
(35) Ding, Y.; Zheng, D.; Xie, L.; Zhang, X.; Zhang, Z.; Wang, L.; Hu, Z.-W.; Yang, Z. Enzyme-instructed peptide assembly favored by preorganization for cancer cell membrane engineering. *J. Am. Chem. Soc.* **2023**, *145* (8), 4366−4371.
(36) Feng, Z.; Wang, H.; Wang, S.; Zhang, Q.; Zhang, X.; Rodal, A. A.; Xu, B. Enzymatic assemblies disrupt the membrane and target endoplasmic reticulum for selective cancer cell death. *J. Am. Chem. Soc.* **2018**, *140* (30), 9566−9573.
(37) Versluis, F.; Van Elsland, D. M.; Mytnyk, S.; Perrier, D. L.; Trausel, F.; Poolman, J. M.; Maity, C.; Le Sage, V. A.; Van Kasteren, S. I.; Van Esch, J. H.; et al. Negatively charged lipid membranes catalyze supramolecular hydrogel formation. *J. Am. Chem. Soc.* **2016**, *138* (28), 8670−8673.
(38) Pires, R. A.; Abul-Haija, Y. M.; Costa, D. S.; Novoa-Carballal, R.; Reis, R. L.; Ulijn, R. V.; Pashkuleva, I. Controlling cancer cell fate using localized biocatalytic self-assembly of an aromatic carbohydrate amphiphile. *J. Am. Chem. Soc.* **2015**, *137* (2), 576−579.
(39) Feng, Z.; Wang, H.; Chen, X.; Xu, B. Self-assembling ability determines the activity of enzyme-instructed self-assembly for inhibiting cancer cells. *J. Am. Chem. Soc.* **2017**, *139* (43), 15377−15384.
(40) Wang, F.; Su, H.; Xu, D.; Dai, W.; Zhang, W.; Wang, Z.; Anderson, C. F.; Zheng, M.; Oh, R.; Wan, F.; et al. Tumour sensitization via the extended intratumoural release of a STING agonist and camptothecin from a self-assembled hydrogel. *Nat. Biomed. Eng.* **2020**, *4* (11), 1090−1101.
(41) Zheng, Z.; Chen, P.; Xie, M.; Wu, C.; Luo, Y.; Wang, W.; Jiang, J.; Liang, G. Cell environment-differentiated self-assembly of nanofibers. *J. Am. Chem. Soc.* **2016**, *138* (35), 11128−11131.
(42) Wang, M. D.; Lv, G. T.; An, H. W.; Zhang, N. Y.; Wang, H. In Situ Self-Assembly of Bispecific Peptide for Cancer Immunotherapy. *Angew. Chem. Int. Ed.* **2022**, *61* (10), No. e202113649.
(43) Jana, B.; Jin, S.; Go, E. M.; Cho, Y.; Kim, D.; Kim, S.; Kwak, S. K.; Ryu, J.-H. Intra-lysosomal peptide assembly for the high selectivity index against cancer. *J. Am. Chem. Soc.* **2023**, *145* (33), 18414−18431.
(44) Jeena, M.; Palanikumar, L.; Go, E. M.; Kim, I.; Kang, M. G.; Lee, S.; Park, S.; Choi, H.; Kim, C.; Jin, S.-M.; et al. Mitochondria localization induced self-assembly of peptide amphiphiles for cellular dysfunction. *Nat. Commun.* **2017**, *8* (1), 26.
(45) Mo, X.; Zhang, Z.; Song, J.; Wang, Y.; Yu, Z. Self-assembly of peptides in living cells for disease theranostics. *J. Mater. Chem. B* **2024**, *12*, 4289.
(46) Chagri, S.; Ng, D. Y.; Weil, T. Designing bioresponsive nanomaterials for intracellular self-assembly. *Nat. Rev. Chem.* **2022**, *6* (5), 320−338.
(47) Liu, H.; Song, Z.; Zhang, Y.; Wu, B.; Chen, D.; Zhou, Z.; Zhang, H.; Li, S.; Feng, X.; Huang, J.; et al. De novo design of self-assembling peptides with antimicrobial activity guided by deep learning. *Nat. Mater.* **2025**, 1−12.
(48) Wu, B.; Yang, X.; Kong, N.; Liang, J.; Li, S.; Wang, H. Engineering Modular Peptide Nanoparticles for Ferroptosis-Enhanced Tumor Immunotherapy. *Angew. Chem. Int. Ed.* **2025**, *64*, No. e202421703.


https://doi.org/10.1021/polymscitech.5c00053
*Polym. Sci. Technol.* XXXX, XXX, XXX−XXX